Vaccine 37 (2019) 6362–6370

Contents lists available at ScienceDirect

Vaccine

journal homepage: www.elsevier.com/locate/vaccine

Identification of mechanisms conferring an enhanced immune response in mice induced by CVC1302-adjuvanted killed serotype O foot-and-mouth virus vaccine

Luping Du [a,b,c,d,1], Xiaoming Yu [a,b,c,d,1], Liting Hou [a,b,c,d], Dong Zhang [e], Yuanpeng Zhang [a,b,c,d], Xuwen Qiao [a,b,c,d], Jibo Hou [a,b,c,d], Jin Chen [a,b,c,d,*], Qisheng Zheng [a,b,c,d,*]

[a] Institute of Veterinary Immunology & Engineering, Jiangsu Academy of Agricultural Sciences, Nanjing, Jiangsu 210014, China
[b] National Research Center of Engineering and Technology for Veterinary Biologicals, Jiangsu Academy of Agricultural Sciences, Nanjing, Jiangsu 210014, China
[c] Jiangsu Co-innovation Center for Prevention and Control of Important Animal Infectious Diseases and Zoonoses, Yangzhou 225009, China
[d] Jiangsu Key Laboratory for Food Quality and Safety-State Key Laboratory Cultivation Base, Ministry of Science and Technology Nanjing, Jiangsu 210014, China
[e] Shandong Provincial Center for Animal Disease Control and Prevention, Jinan, Shandong 250022, China

ARTICLE INFO

Article history:
Received 3 June 2019
Received in revised form 26 August 2019
Accepted 5 September 2019
Available online 13 September 2019

Keywords:
FMDV
CVC1302
Local mechanism
Injection sites
Draining lymph nodes
Mice

ABSTRACT

The adjuvant CVC1302 was previously shown to efficiently enhance the immunogenicity of killed foot-and-mouth disease virus (FMDV) in mice and piglets. However, the underlining mechanism of action of CVC1302 remains unclear, especially at local injection sites and draining lymph nodes. Since the FMDV vaccine is administrated intramuscularly in field settings, we studied local immune responses to FMDV following intramuscular injection in mice, and found that CVC1302-adjuvanted killed FMDV (KV-CVC1302) induced secretion of several chemokines in murine muscle tissues, including MCP-1, MIP-1α, and MIP-1β. The number of monocytes recruited to the site of injection was significantly higher in mice immunized with KV-CVC1302 compared with mice immunized with killed FMDV alone (KV). iTAQ-based quantitative proteomic assays were additionally employed to explore the molecular mechanisms of CVC1302 action in the draining lymph nodes. A total of 35 proteins were identified as being differentially expressed among the control group, KV-immunized group and KV-CVC1302-immunized group at 10 days post immunization (dpi). Proteins exhibiting differential expression were mainly involved in signal transduction, apoptosis, endocytosis and innate immune responses. Pathway analysis demonstrated that AMPK, phospholipase D, cAMP, Rap1, and MAPK signaling pathways were potentially induced by the immunopotentiator CVC1302. Understanding the local mechanism of CVC1302 action at injection sites and draining lymph nodes will provide new insights into the development of FMDV vaccines.

1. Introduction

Foot-and-mouth disease (FMD), caused by foot-and-mouth disease virus (FMDV), is an economically devastating infection of wild and domestic cloven-hoofed animals [23]. FMDV belongs to the family *Picornaviridae* and has a single-stranded, positive-sense RNA genome [21]. In China, FMDV serotype O is currently prevalent, and disease control relies mainly on vaccination with killed vaccines [13]. However, the inherent disadvantages of killed FMDV vaccines, such as a short duration of immunity, the need for repetitive vaccination, and partial immune protection, limit their application and use [2].

In our previous study, a complex of muramyl dipeptide (MDP), monophosphoryl lipid A (MPL) and β-glucan called CVC1302 was used to improve the efficacy of a killed FMDV serotype O vaccine [9]. Significantly higher titers of liquid-phase blocking (LPB) antibodies were induced in pigs immunized with CVC1302-adjuvanted killed FMDV (KV-CVC1302) compared with KV alone. Long-lasting humoral immunity was confirmed as efficient LPB antibody titers in pigs were elicited after only a single dose of KV-CVC1302. Moreover, we showed through challenge experiments that KV-CVC1302 vaccine could provide efficient protective immunity in pigs against FMDV infection. Therefore, deciphering

* Corresponding authors at: Institute of Veterinary Immunology & Engineering, Jiangsu Academy of Agricultural Sciences, Nanjing, Jiangsu 210014, China.
E-mail addresses: chenjin_abc@163.com (J. Chen), immun_tech@163.com (Q. Zheng).
[1] These authors contributed equally to this work.

https://doi.org/10.1016/j.vaccine.2019.09.014
0264-410X/

the mechanism of CVC1302 adjuvant in improving responses against killed FMDV vaccines represents an urgent priority. As local events at injection sites represent critical steps towards mounting a robust immune response, we sought to elucidate the molecular mechanisms of CVC1302 action at murine injection sites.

Prior studies have demonstrated that long-term humoral immunity induced by CVC1302-adjuvanted serotype O FMDV killed vaccine correlates with promoted T follicular helper cells, and thus germinal center responses in mice. This is in agreement with studies in the literature which have reported that exposure of murine B cells to TLR4, TLR7, and TLR9 agonists increases the expression of B cell costimulatory factors and induces B cells to proliferate, produce cytokines, differentiate into APCs, switch Ig classes, and secrete Igs [18,33]. As CVC1302 is comprised of MDP, MPL and β-glucan, which are TLR agonists, we utilized iTAQ-based quantitative proteomic assays to explore whether CVC1302 adjuvant improves serotype O FMDV killed vaccine through B cell-intrinsic MyD88 signaling. Our findings support the need for further study of local host responses elicited by KV-CVC1302 at injection sites in pigs to fully understand the mechanism of action of killed FMDV vaccines.

2. Materials and Methods

2.1. Mice

Seventy-eight six-week-old female pathogen-free BALB/c mice purchased from the Yang Zhou University were divided into three experimental groups. The study and protocol were both approved by the Science and Technology Agency of Jiangsu Province (the approval number is NKYVET 2015-0066) and by the Jiangsu Academy of Agricultural Sciences Experimental Animal Ethics Committee. All efforts were made to minimize animal suffering. All animal studies were performed in strict accordance with the guidelines of Jiangsu Province Animal Regulations (Government Decree No. 45).

2.2. Antigen, adjuvants, and immunizations

Killed FMDV serotype O was a kind gift from China Agricultural Vet. Bio. Science and Technology Co. Ltd. (CAVI, Lanzhou, China). CVC1302 was prepared by dissolving MDP, MPL, and β-glucan in sterile water. These adjuvants were prepared as described in the Chinese patent license (registered number 201310042983.0, see Supplemental data). One volume of adjuvant was thoroughly mixed with nine volumes of killed FMDV, and then combined with an equal volume of a Montanide IMS 1313™ N VG (Seppic, France) prior to injection. The killed FMDV vaccine mixed with CVC1302 and Montanide IMS 1313™ N VG was called KV-CVC1302. The killed FMDV vaccine mixed with Montanide IMS 1313™ N VG alone was called KV.

All groups of mice were injected intramuscularly (i.m.) with 50 μL of antigen-adjuvant mixture in the quadriceps muscle of each hind leg (100 μL/mouse). Group 1 mice (n = 26) were injected once with Montanide IMS 1313™ N VG alone as a negative control. Group 2 mice (n = 26) were injected once with KV (0.3 μg killed FMDV per animal). Group 3 mice (n = 26) were injected once with KV-CVC1302 (0.3 μg killed FMDV per animal).

Samples from injection sites (hind leg quadriceps) and draining lymph nodes were collected at 0, 1, 3, 5, 7 and 14 dpi from immunized mice to analyze antigen presenting cells (APCs). Three mice in each group were sacrificed at each time point. At 1 dpi, the sera and muscles of three mice from each group were collected to analyze cytokine expression. For confocal microscopy, the muscles of three mice from each group were collected at 6 h (h) after immunization. For iTRAQ-based quantitative proteomic assays, inguinal lymph nodes of individual mice (two mice in each group) were collected at 10 dpi and stored at −80 °C until use.

2.3. Cytokine analysis

Cytokine concentrations in muscle samples were measured at 1 dpi with KV, KV-CVC1302 or vehicle control vaccinated mice. Muscles were homogenized in native lysis buffer (Solarbio, Beijing) containing 10 μM phenylmethanesulfonyl fluoride (PMSF) (Solarbio, Beijing) with an Ultra-Turrax T25 instrument. Homogenates were centrifuged at 10,000*g* for 10 min at 4 °C and total protein concentrations in the supernatants were determined using a bicinchoninic assay kit (Solarbio, Beijing). Muscle tissue homogenates were diluted with buffer to a protein concentration of 500 μg/mL and cytokine concentrations were measured using commercial ELISA kits (Miltenyi, Germany).

Additionally, the concentrations of IFNs and MCP-1, MIP-1α, MIP-1β in sera were also measured by using commercial ELISA kits (Miltenyi, Germany) according to manufacturer's instructions. The cytokine concentrations in the samples were determined based on the standard curves.

2.4. Quantitative real-time PCR (qPCR)

Total RNA was extracted from muscle tissues using Trizol (Invitrogen, USA) and reverse transcribed in a 20 μL volume using a Prime Script TM II Strand cDNA Synthesis kit (Takara, Dalian, China), according to the manufacturer's protocol. The cDNA product (2 μL) was amplified in a 20 μL qPCR reaction mixture containing Bright Green 2× qPCR Master Mix (abm, Canada) and 0.2 μM of each of the forward and reverse gene-specific primers. Each cDNA amplification was performed in triplicate. PCR amplifications were performed using a Roche Light Cycler®480 instrument. The thermal cycling conditions were as follows: 10 min at 94 °C, 40 cycles of 15 s at 94 °C and 1 min at 60 °C. Gene expression was measured by relative quantity as described previously [14]. The primers used in this study are listed in supplemental Table 1.

2.5. Preparation of single-cell suspensions from injection sites and draining lymph nodes

Quadriceps muscles were harvested and placed in tissue culture dishes containing Hank's Balanced Salt Solution (HBSS; Gibco) on ice [7]. The muscles were cut into small pieces and digested with 0.05% (w/v) type II collagenase (Sigma) in HBSS for 30 min at 37 °C with constant agitation. The cell suspension was centrifuged at 400*g* for 5 min, resuspended in Dulbecco's Modified Eagle's Medium (DMEM; Gibco), filtered through a 70 μm nylon mesh (BD Falcon, USA) and stained with fluorescent labeled antibodies for flow cytometric analysis.

Draining lymph nodes were harvested and cut into small fragments. Single lymphocytes were prepared using a Medimachine system with a Medicon (50 μm) disaggregator (BD, USA) and stained with fluorescent-labeled antibodies for flow cytometric analysis.

2.6. Flow cytometric analysis

Cells were stained with combinations of the following antibodies: anti-CD11b PE-Cy7 (clone M1/70; BD Biosciences, USA), anti-CD11c FITC (clone N418; Miltenyi Biotec, USA), anti-Ly6G PE (clone 1A8; BD Biosciences, USA), anti-Ly6C APC (clone HK1.4; Invitrogen, USA), anti-F4/80 PE (clone REA126; Miltenyi Biotec, USA), anti-MHC class II APC (clone REA610; Miltenyi Biotec,

USA), anti-CD80 APC (clone 16-10A; Mitenyi Biotec, USA), anti-CD86 APC (clone PO3.3; Mitenyi Biotec, USA) and anti-CD40 APC (clone FGK45.5; Miltenyi Biotec, USA).

Cells were analyzed with a BD Accuri C6 instrument (BD Biosciences, USA). Data analyses were performed using FlowJo version 7.6.1 software.

2.7. Confocal microscopy

Tissue samples from injection sites (quadriceps muscles) of three different mice were collected 6 h after immunization and immediately frozen using liquid nitrogen according to the procedure described by Kasturi et al. with some modifications [24]. Opti-

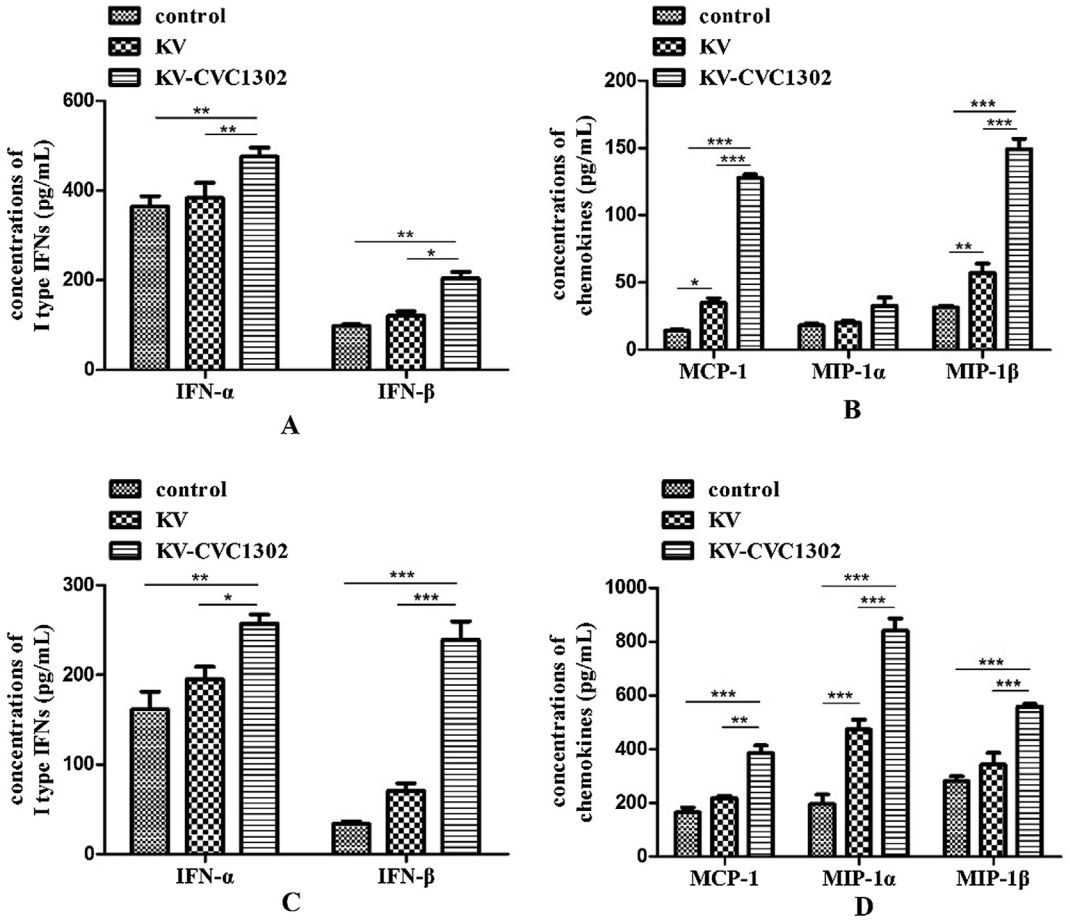

Fig. 1. Expression of cytokines and chemokines measured by ELISA in sera and at injection sites after immunization with vehicle alone, KV or KV-CVC1302. The immunization protocol is described in the Materials and Methods. Serum and muscle samples from the injection sites were collected at 1 dpi to quantitate type I IFNs (A, C) and chemokines (MCP-1, MIP-1α and MIP-1β) (B, D). Data are presented as the mean ± SEMs.

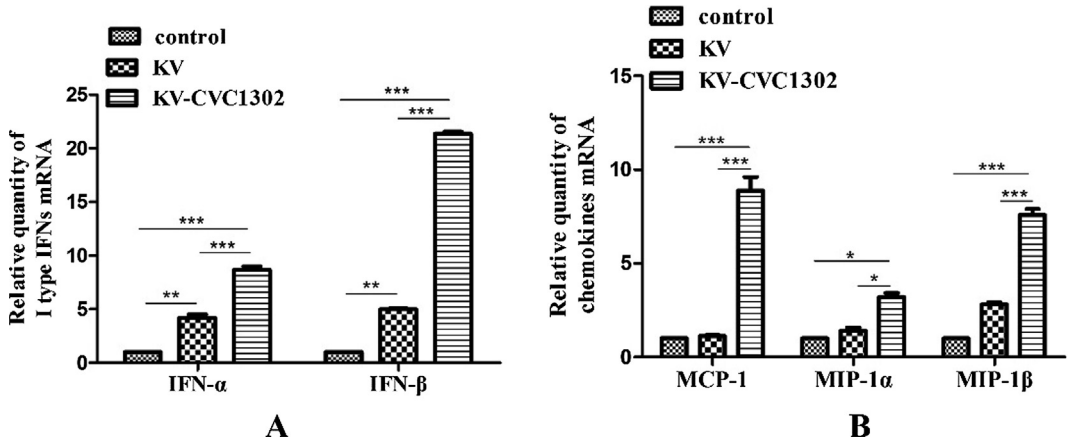

Fig. 2. Abundance of mRNA transcripts encoding cytokines and chemokines at injection sites after immunization with vehicle alone, KV or KV-CVC1302. The immunization protocol is described in the Materials and Methods. Injected muscle samples were collected at 1 dpi to quantitate type I IFNs (A) and chemokines (MCP-1, MIP-1α and MIP-1β) (B). Data are presented as the mean ± SEMs.

mal cutting temperature compound (OCT) (Leica Microsystems, Wetzlar, Germany)-embedded muscle tissue was sectioned transversely at 6 μm by using a CM1950 cryostat (Leica Microsystems, Wetzlar, Germany). Tissue samples were captured on Superfrost plus microscope slides (Thermo Scientific, USA) and washed with phosphate-buffered saline (PBS) three times to remove any residual OCT. The cryosections were fixed using PBS containing 3% formaldehyde for 10 min at room temperature, washed twice with PBS, and permeabilized with PBS containing 3% bovine serum albumin (BSA) and 1% saponin (permeabilization buffer) for 30 min at room temperature. Tissue sections were stained with anti-CD11c FITC and 4′,6′-diamidino-2-phenylindole (DAPI) for 1 h at room temperature in the dark. Sections were visualized and photographed with a Zeiss LSM700 confocal microscope (objective, 320 nm) at room temperature and images were acquired with Zeiss LSM image browser software (Zeiss). The images were then examined with image analysis software Image-Pro Plus 6.0.

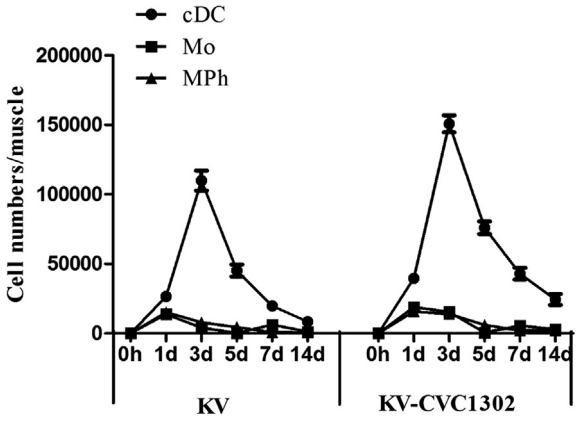

Fig. 3. Kinetics of cell recruitment to sites of injection in muscle tissue following KV-CVC1302-injection. The immunization protocol is described in the Materials and Methods. The cell composition at injection sites in muscles was assessed at the indicated time points by flow cytometry. Values show mean ± SEMs of 4–6 muscles from 2 to 3 mice per treatment group.

2.8. iTRAQ-based quantitative proteomic assays

2.8.1. Protein extraction, digestion and iTRAQ labeling

Frozen samples were transferred into low protein binding tubes (1.5 mL) and lysed with 500 μL digestion buffer supplemented with 1 mM PMSF. Then, the tissue samples were homogenized on ice and further lysed with sonication. After sonication, the samples were centrifuged at 15,000 g for 15 min at 4 °C to remove insoluble particles, and repeated once to further exclude insoluble particles. Protein digestion was conducted according to the FASP procedure described by Wisniewski et al. [43]. For iTRAQ labeling, the resulting peptide mixture was then labeled with iTRAQ reagent (Applied Biosystems, Carlsbad, CA, USA), according to the manufacturer's instructions. Two hundred microliters of isopropanol was added to each room-temperature iTRAQ reagent vial. Then, 100 μL of the iTRAQ labeled reagent was added to each sample for mixing. The tubes were incubated at room temperature for 2 h. Finally, 200 μL of HPLC water was added to each sample and incubated for 30 min to terminate the reaction. The samples were lyophilized and stored at −80 °C.

2.8.2. Reverse phase fractionation and Nano LC-MS/MS analysis by Q Exactive

Reverse phase (RP) separation and Nano LC-MS/MS analysis were performed according to protocols described in Xu et al. [44]

2.8.3. Database search

Proteome Discoverer (v.2.2) was used to search all of the Q Exactive raw data thoroughly against the sample protein database. Database searches were performed with Trypsin digestion specificity. Alkylation on cysteine was considered a fixed modification in the database search. For protein quantification method, iTRAQ 8 plex was selected. A global false discovery rate (FDR) was set

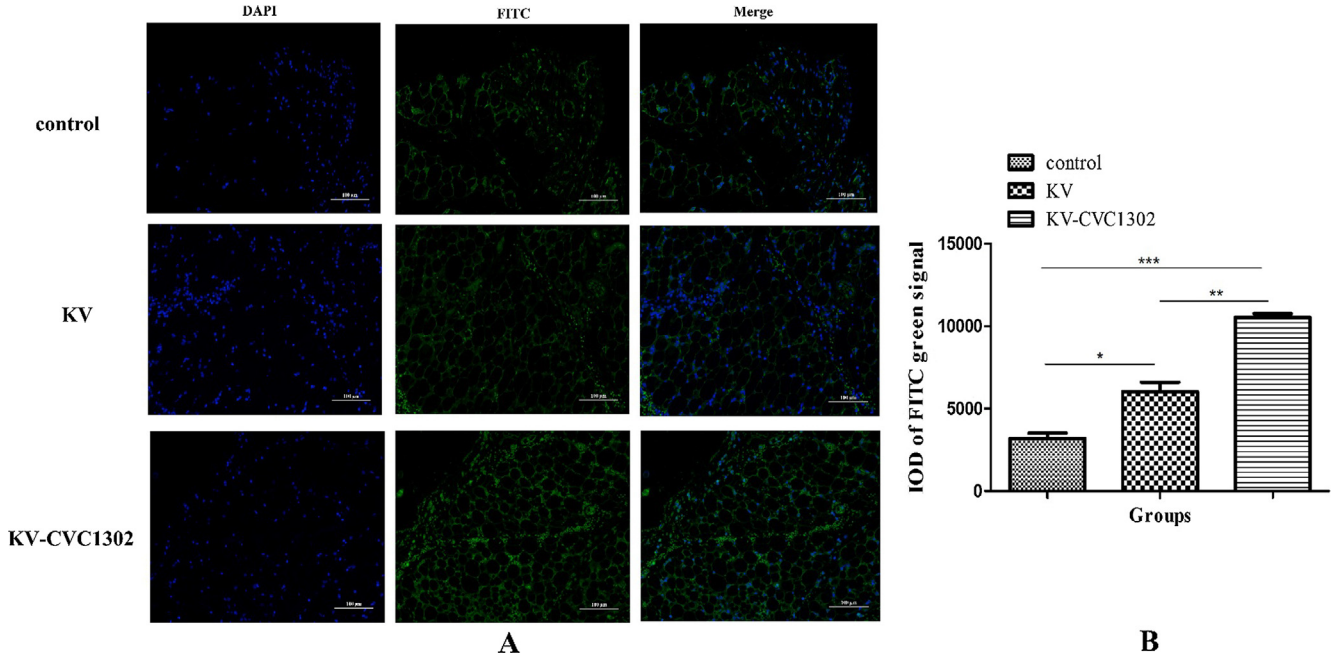

Fig. 4. (A) Confocal microscopy of muscle cryosections 6 h after immunization. CD11c$^+$ cells are shown in green and nuclei (DAPI) are shown in blue. Muscle tissues sampled from mice immunized with control, KV or KV-CVC1302. Magnification, 200×. (B) The integral optical density (IOD) analysis of injected muscles on FITC signal. (For interpretation of the references to color in this figure legend, the reader is referred to the web version of this article.)

to 0.01 and protein groups considered for quantification required at least 2 peptides.

2.9. Statistical analysis

Statistical analysis was performed using GraphPad Prism version 5 (GraphPad Software, San Diego, CA, USA). Differences among groups were assessed using one-way analysis of variance (ANOVA) with post-hoc Tukey's and Student's *t*-tests. *P* values less than 0.05 were considered as statistically significant. All data were expressed as means ± standard error of the means (SEMs).

3. Results

3.1. Efficient induction of cytokines and chemokines by CVC1302

As CVC1302 is a complex of several Toll-like receptor (TLR) agonists, which mainly induces type I interferons (IFNs), we first assessed cytokine levels in the sera of mice at 1 dpi with either vehicle alone, KV or KV-CVC1302, using commercial ELISA kits. As shown in Fig. 1A, immunization with KV-CVC1302 induced significantly higher levels of IFNα and IFNβ than immunization with KV alone.

Levels of IFNs were also measured locally using commercial ELISA kits and qPCR. As shown in Fig. 1C, enhanced expression of IFNα and IFNβ at injection sites was observed in mice immunized with KV-CVC1302. Consistent with ELISA results, there was a significant difference between mice immunized with KV alone or KV-CVC1302 with regard to IFNα and IFNβ mRNA expression levels at injection sites (Fig. 2A).

Previous studies have shown that adjuvants, such as MF59 and Alum, primarily improve vaccine efficacy by inducing chemokine secretion to recruit immune cells, especially APCs, to sites of immunization [7]. Accordingly, we investigated chemokine levels induced in both injection sites and sera of KV- and KV-CVC1302-immunized mice to determine whether CVC1302 functioned similarly to improve the efficacy of FMDV vaccines. We found that elevated levels of the monocyte chemoattractant protein-1 (MCP-1 or CCL2), macrophage inflammatory protein-1α (MIP-1α or CCL3) and macrophage inflammatory protein-1β (MIP-1β or CCL4) could be detected in sera and at injection sites of mice immunized with KV-CVC1302 (Fig. 1(B and D)), with the elevated levels of MCP-1, MIP-1α and MIP-1β mRNA additionally detected at injection sites (Fig. 2B). In contrast, compared with mice immunized with KV-CVC1302, mice from control or KV groups only possessed low levels of MCP-1, MIP-1α and MIP-1β. The primary roles of MIP-1α and MIP-1β are to recruit MPh, which capture injected antigens in order to activate immune responses [6,8,17]. MCP mainly attracts Mo, which can differentiate into DCs and play a crucial role in antigen uptake and subsequent stimulation of adaptive immunity [4,16,36]. In our study, significantly elevated levels of DCs were observed in mice 3 dpi with KV-CVC1302 compared with KV. For these reasons, we speculate that CVC1302 might induce Mo differentiation into DCs, although further studies will be required to explore this possibility.

Collectively, we found that CVC1302 induced not only elevated levels of type I IFNs to improve the efficacy of killed FMDV vaccine, but also elevated chemokine secretion in order to recruit APCs to capture and present antigens.

3.2. Recruitment of cells to the injection site in quadriceps muscles

Given the chemokine profile in KV-CVC1302-immunized mice, we next analyzed cellular recruitment (specifically APCs) to the injection site using flow cytometry. Single-cell suspensions were obtained by enzymatic digestion of muscle tissue. Using specific antibodies recognizing cell type-specific markers, we detected cDC ($CD11b^+$, $CD11c^+$), macrophages (MPh) ($CD11b^+$, $CD11c^-$, $F4/80^{high}$), and monocytes (Mo) ($CD11b^+$, $CD11c^-$, $Ly6C^+$, $Ly6G^-$). As shown in Fig. 3, significantly higher numbers of dendritic cells (DCs) were observed at sites of injection in mice immunized with KV-CVC1302 compared with mice immunized with KV alone, most notably at 3 dpi. Peak numbers of recruited DCs at injection sites were observed at 3 dpi in both mice immunized with KV-CVC1302 or KV alone, as MPh and Mo were at 1 dpi. No significant difference in the number of MPh and Mo recruited to injection sites was observed at 7 dpi, or Mo at 1 and 14 dpi; however, enhanced numbers of Mo were recruited to the injection sites of KV-CVC1302-immunized mice at 3 dpi, which may in part explain the enhanced numbers of DCs detected on subsequent days. Recruited Mo may have, in turn, recruited DCs or differentiated into DCs themselves. Statistical analysis supporting these conclusions are shown in the supplemental Table 2.

Injection sites in quadriceps muscles of KV-CVC1302- and KV-immunized mice were observed by confocal microscopy at 6 h post immunization to further analyze the recruitment of DCs. As shown in Fig. 4A and B, significantly more CD11c+ DCs (green fluorescence) were observed in the muscle tissue samples from

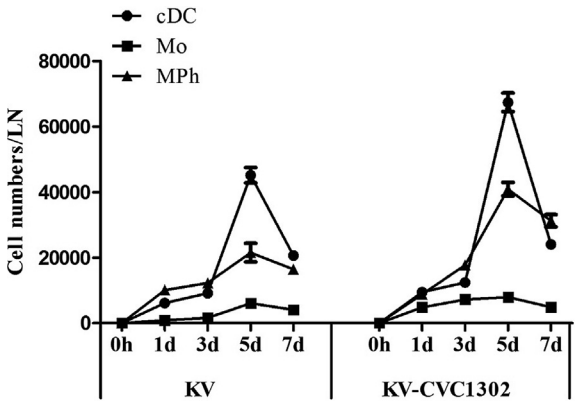

Fig. 5. Kinetics of cell recruitment into the draining lymph nodes in response to immunization with KV-CVC1302. The immunization protocol isdescribed in the Materials and Methods. The cell composition in the lymph nodes of all mice was assessed at the indicated time points by flow cytometry. Values show mean ± SEMs of 4–6 lymph nodes from 2 to 3 mice per treatment group.

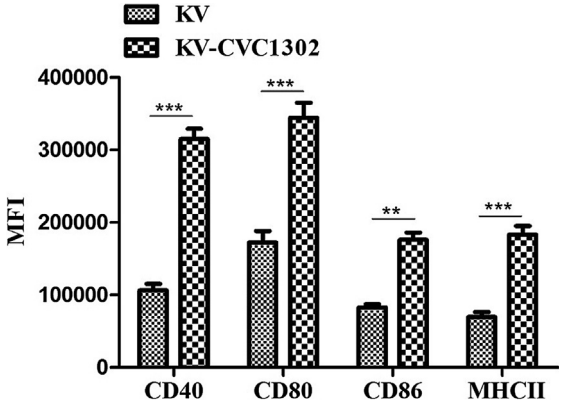

Fig. 6. Activation of recruited DCs ($CD11b^+$, $CD11c^+$) at sites of injection in muscle tissues of mice immunized with KV or KV-CVC1302. The immunization protocol is described in the Materials and Methods. The cell-surface expression of CD40, CD80, CD86 and MHCII on DCs was assessed by flow cytometry.

KV-CVC1302-immunized mice compared with mice immunized with KV alone.

Concurrently, the numbers of APCs in draining inguinal lymph nodes were analyzed by using flow cytometry. Similar to the injection site, DCs had the highest frequency among all APCs in both groups of mice immunized with KV-CVC1302 and KV alone (Fig. 5). The highest numbers of APCs among all types were detected at 5 dpi in the inguinal lymph nodes from both groups immunized with KV-CVC1302 and KV alone (statistical analysis is shown in the supplemental Table 3).

Collectively, these data show that, as elevated chemokine secretion was induced by CVC1302, higher numbers of APCs, including DC, MPh and Mo, were recruited to the site of injection to capture more antigens and transfer them to inguinal lymph nodes in order to activate efficient germinal center reactions.

3.3. Activation of DCs recruited to sites of injection

DC recruitment to the injection site is a critical first step in the activation of immune responses following vaccination. Furthermore, efficient activation of recruited DCs is important for antigen processing and presentation [39,35]. TLRs have been shown to play an essential role in activation of DCs [1,34,26], CVC1302 is a complex of TLR ligands. As such, we next analyzed DC activation via flow cytometry. As shown in Fig. 6, significantly higher levels of CD40, CD80, CD86 and MHCII expression were observed on DCs from mice immunized with KV-CVC1302 compared with mice immunized with KV alone. Enhanced expression levels of CD80, CD86 and MHCII among DCs may have promoted their ability to process and present antigen to T or B cells.

3.4. GO and KEGG pathway analysis of DEPs

To more comprehensively explore complex host responses following immunization, we employed iTRAQ technology to analyze the proteomics of mice inoculated with vaccine vehicle, KV or KV-CVC1302. Based on the database of *Mus musculus.* fasta, 1942 proteins (≥one or more unique peptides with an FDR less than 1%) were identified.

Thirty-five differentially expressed proteins (DEPs) (upregulated ≥ 1.2-fold or downregulated ≤ 0.84-fold; $P \leq 0.05$) were selected in inguinal lymph nodes from groups of mice immunized with vaccine vehicle, KV or KV-CVC1302, respectively. A hierarchical clustering heat map of the DEPs is shown in Fig. 7.

The DEPs identified above were classified according to their biological processes, cellular components and molecular functions using the OmicsBean database; their relative classifications are listed in Fig. 8. According to this comprehensive analysis, we found that most of the DEPs were associated with apoptosis, autophagy, germinal center processes, and regulation of immune responses (Table 1), which might be associated with the adjuvanticity of the immunopotentiator CVC1302.

Among the DEPs, we found that Nmi, which was responsible for negative regulation of type I IFNs [41,12,22], was down-regulated in the groups of mice immunized with KV-CVC1302 or KV compared with mice immunized with PBS. Furthermore, the abundance of Nmi in KV-CVC1302–immunized mice was statistically lower than in mice immunized with KV, which was related to the components of CVC1302, a complex of several Toll-like receptor (TLR) agonists. These results were consistent with our aforementioned observation that the levels of type I IFNs at injection sites and in the sera of mice in the KV-CVC1302 group were higher than levels detected in the KV group. Moreover, we found that the levels of Clec2d and Gbf1 in lymph nodes sampled from mice immunized with KV-CVC1302 were significantly higher than mice immunized with KV (both $p < 0.05$); this is in agreement with prior

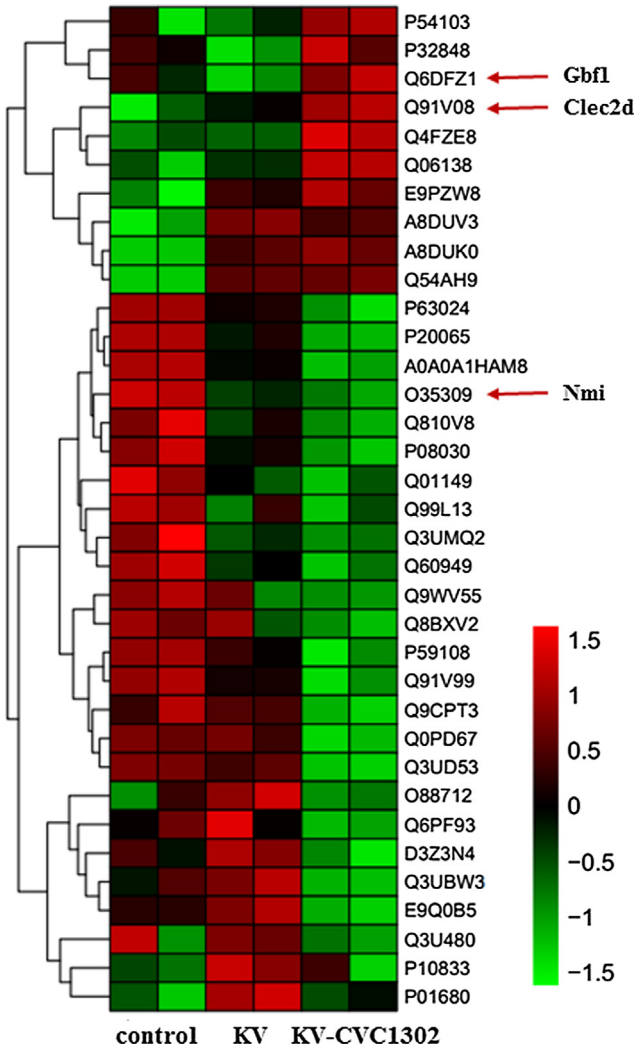

Fig. 7. Heat map of differentially expressed proteins (DEPs) in inguinal lymph nodes from KV or KV-CVC1302-treated and control mice at 10 dpi. Each column represents an experiment sample. Color legend is on the right, the color scale ranges from saturated green for log ratios −1.5 and above to saturated red for log ratios 1.3 and above. Red indicates increased protein expression levels; green indicates decreased levels compared with control samples. (For interpretation of the references to color in this figure legend, the reader is referred to the web version of this article.)

studies which have demonstrated known roles for these proteins in the regulation of immune responses [19,25,27,5]. Briefly, Gbf1 was identified to play an important role in cell activation involved in immune responses, and it was demonstrated that Clec2d triggering may play a key role in germinal center (GC) reactions promoting B cell activation and downregulating CXCR4, thus helping to promote an LZ phenotype and facilitating both FDC and Tfh interactions. Considering this past work, we speculate that CVC1302 may induce high levels of Gbf1 and Clec2d to improve the immune responses induced by killed FMDV vaccine.

Based on the results of iTAQ-based quantitative proteomic assays, we found that Pik3c3 [46], Colla2 [45], Rab1a [42], Rps6ka1 [38], Tbc1d1 [40], Vapa [47], Vamp3 [29,15], Marck3 [32] and Cpne2 [10] were down-regulated in inguinal lymph nodes sampled from mice immunized with KV-CVC1302 compared with mice receiving KV alone.

Furthermore, as shown in Fig. 9, the AMPK signaling pathway plays several important roles in cell proliferation, apoptosis and autophagy [28]. In GC reactions, following proliferative expansion

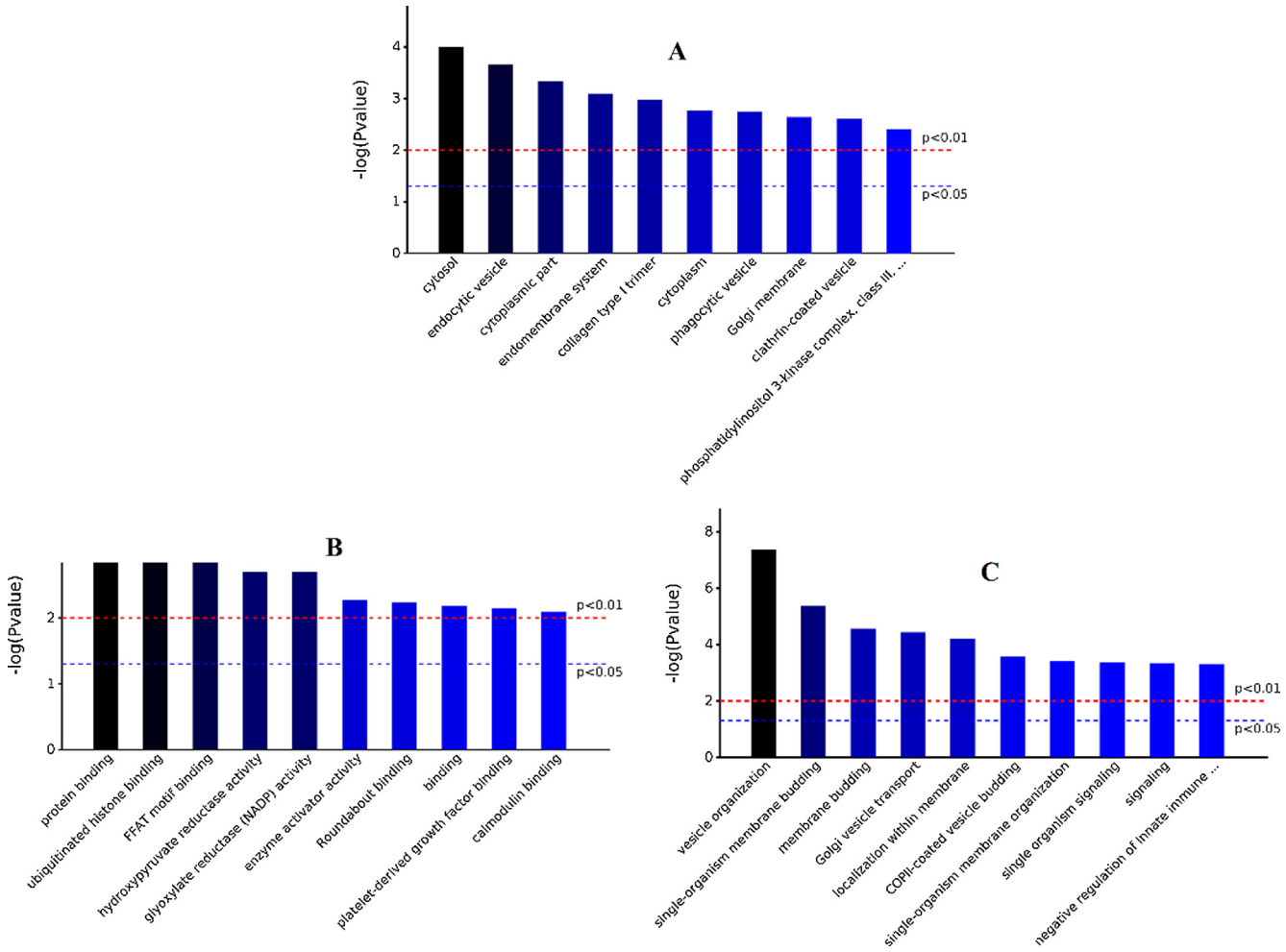

Fig. 8. Gene ontology (GO) annotation of DEPs in inguinal lymph nodes from KV or KV-CVC1302-treated and control mice at 10 dpi. Functional analysis of the proteins included three categories: cellular component (A), molecular function (B) and biological process (C).

Table 1
The GO and KEGG analysis of the main DEPs.

Protein ID	Gene	Abundance						References	GO and KEGG analysis
		Group1		Group2		Group3		PMID/PMCID	
Q6PF93	Pik3c3	102.4	112.5	124.3	102.2	83.1	85.3	24013218	Phagosome
Q01149	Colla2	132	121.1	102.5	90.6	77	91.3	30123364	PI3K-Akt signaling pathway
Q0PD67	Rabla	109.8	108.2	109.3	104.8	83.5	85.7	27334615	Autophagosome organization
Q810V8	Rps6kal	117.3	128	98.9	107.7	91.5	87.8	21035469	Apoptosis
Q60949	Tbc1d1	116.7	122.4	92.6	98.9	76.9	86	30135087	AMPK signaling pathway
Q9WV55	Vapa	109.5	112.1	107.5	92.9	92.4	91.8	29628370	Autophagosome
P63024	Vamp3	111.9	111.9	102.2	103.2	91.6	86.5	25046144	Phagosome
A0A0A1HAM8	Marcks	107.9	108.5	98.4	99.4	88.7	90.3	26470024	Phagosome
P59108	Cpne2	109.9	111	104.2	100.9	85.8	91.7	PMC6227306	Autophagosome clearance
Q3UD53	CARHSP1	108.4	107.8	103.8	106	85	84.1	21078874	TNF-α protein production
O88712	Ctbp1	89.6	106.9	114.5	120.4	89.4	91.7	18212045	Transcription of Bcl-6
O35309	Nmi	122.9	121.3	96.9	99.6	91.4	86.7	26342464	Negative regulation of I type IFN expression
Q6DFZ1	Gbf1	104.1	98	88.3	92.2	107.2	111.2	28702273	Cell activation involved in immune response
Q91V08	Clec2d	81.8	91.9	99.2	97.1	111.8	110	27626681	Regulation of immune response
Q06138	Cab39	90.3	78.8	93.2	93.5	115.6	114.4	28628644	AMPK signaling pathway
E9PZW8	Myo9b	86.9	76.1	104.9	102.4	116	108.9	24646736	Endocytosis

and somatic hypermutation (SHM) in the dark zone, B cells move to the light zone where those that have high affinity for the antigen are selected for survival, re-enter the dark zone or differentiate to memory B cells and plasma cells. However, low-affinity GC B cells are selected for apoptosis [3].The finding may partially explain that CVC1302 enhances murine IgG responses against FMDV by promoting the magnitude of GC B cell responses [13]. Significant differences in phagosome and regulation of autophagy were discovered among the groups of mice immunized with vaccine vehicle, KV or KV-CVC1302.

As the germinal center response peaks between day 10 and day 14 after immunization and then diminishes [37], we sampled

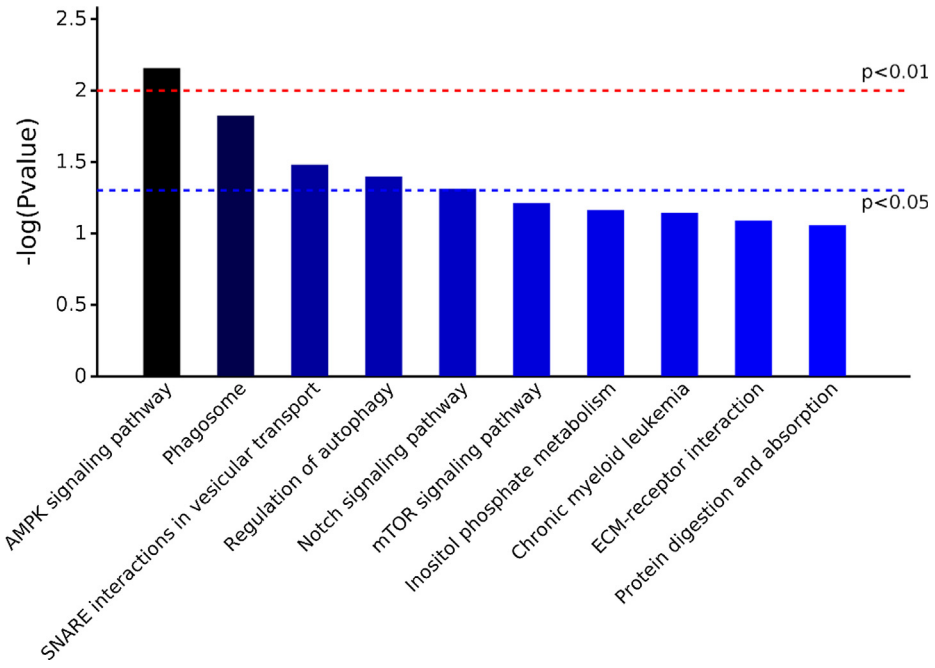

Fig. 9. KEGG pathway associated with the DEPs in inguinal lymph nodes from KV or KV-CVC1302-treated and control mice at 10 dpi. Top 10 enrichment in KEGG pathway maps of the DEPs.

inguinal lymph nodes from mice immunized with vehicle, KV or KV-CVC1302 at 10 dpi, to analyze the ability of CVC1302 to improve immune responses induced by FMDV killed vaccine. iTRAQ analysis not only identified elevated levels of type I IFNs in mice immunized with KV-CVC1302, but also demonstrated that CVC1302 plays important roles in the regulation of the magnitude of GC reactions through promoting B cell activation, facilitating both FDC and Tfh interactions and regulating the GC reaction process.

4. Discussion

FMD, one of the most contagious viral diseases of livestock, causes substantial economic losses worldwide [21]. In China, immunization with killed FMDV vaccine represents the primary method for FMD control and prevention [31]. Currently, the commercially-used killed FMDV vaccine usually requires 7–10 days to elicit protective immunity and does not confer long-lasting immunity [20,11,30]. Typically, multiple vaccinations with conventional killed FMDV vaccine are required to induce adequate immunity; therefore, a single adjuvanted FMDV vaccination approach would provide a substantial advantage. In our previous study, we found that CVC1302 adjuvant could improve the efficacy of a killed FMDV vaccine in pigs, inducing elevated LBP-antibody levels and neutralizing antibodies titers [9]. LBP-ELISA has many advantages in evaluating vaccine-induced immunity and serological diagnosis, and has become a standard method for detecting serum antibody of FMDV in China. While LBP-ELISA titer is a common detection method available for the evaluation of FMD vaccine, detection of neutralizing antibodies must be performed by the designated laboratories in China due to safety regulations, so only LBP antibody titers induced by KV-CVC1302 were evaluated here. In this study, we sought to understand the mechanism of CVC1302 adjuvant functionality at injection sites with a killed FMDV serotype O vaccine in the mouse model, as mice serve well as an in vivo model for vaccine efficacy studies due to an abundance of species-specific immunological reagents, a well-studied genomic background, and low cost. By using flow cytometry and iTRAQ approaches, we demonstrated that CVC1302 could not only induce elevated type I IFNs and chemokines (MCP-1, MIP-1α and MIP-1β) at injection sites and in sera to activate immune response against FMDV, but could also improve GC reactions to produce higher levels of FMDV-specific LBP antibody through promoting B cell activation, facilitating both FDC and Tfh interactions and regulating the GC reaction process. The results from our investigation of CVC1302 efficacy in the mouse model warrant further examination of this adjuvant in pigs.

CVC1302 is a complex of MDP, MPL, and β-glucan; in this study, we explored the mechanism of action of this adjuvant as a complex, but did not examine the individual components in isolation. However, based on the results of this study, further studies to explore the contribution of the individual components of CVC1302 in improving the efficacy of KV are planned.

Montanide IMS 1313™ N VG, an oil-in-water formulation, was used in this study to encapsulate killed FMDV either alone or in combination with CVC1302. The vehicle alone group was immunized with Montanide IMS 1313™ N VG diluted in PBS, to control for any effects of Montanide IMS 1313™ N VG, as all of the immunized animals received Montanide IMS 1313™ N VG.

In summary, our study identified that the mechanism of CVC1302 mainly relies on enhancing the expression of chemokines (MCP, MIP-1α and MIP-1β) to improve the recruitment of DCs, Mo and MPh to the sites of KV injection. The overall effect involves increased capture, processing and presentation of injected antigen to T or B cells to activate immune responses. Furthermore, iTAQ-based quantitative proteomic assays showed that CVC1302 not only modulates the expression of I type IFNs, but also promotes the magnitude of GC reactions in inguinal lymph nodes. Collectively, these findings provide novel insights towards the development of a new generation of immunopotentiators compatible with FMDV vaccine.

Declaration of Competing Interest

The authors declare that they have no known competing financial interests or personal relationships that could have appeared to influence the work reported in this paper.

Acknowledgements

This work was supported by the National Natural Sciences Foundation of China (31802220). We thank Liwen Bianji, Edanz Editing China (www.liwenbianji.cn/ac), for editing the English text of a draft of this manuscript.

Disclosures

The authors have no financial conflicts of interest.

Appendix A. Supplementary data

Supplementary data to this article can be found online at https://doi.org/10.1016/j.vaccine.2019.09.014.

References

[1] Adema GJ. Dendritic cells from bench to bedside and back. Immunol Lett 2009;122:128–30.
[2] Barteling SJ, Vreeswijk J. Developments in foot-and-mouth disease vaccines. Vaccine 1991;9:75–88.
[3] Basso K, Dalla-Favera R. Germinal centres and B cell lymphomagenesis. Nat Rev Immunol 2015;15:172–84.
[4] Boring L, Gosling J, Chensue SW, Kunkel SL, Farese Jr RV, Broxmeyer HE, et al. Impaired monocyte migration and reduced type 1 (Th1) cytokine responses in C-C chemokine receptor 2 knockout mice. J Clin Invest 1997;100:2552–61.
[5] Busby T, Meissner JM, Styers ML, Bhatt J, Kaushik A, Hjelmeland AB, et al. The Arf activator GBF1 localizes to plasma membrane sites involved in cell adhesion and motility. Cell Logist 2017;7:e1308900.
[6] Bystry RS, Aluvihare V, Welch KA, Kallikourdis M, Betz AG. B cells and professional APCs recruit regulatory T cells via CCL4. Nat Immunol 2001;2:1126–32.
[7] Calabro S, Tortoli M, Baudner BC, Pacitto A, Cortese M, O'hagan DT, De Gregorio E, Seubert A, Wack A. Vaccine adjuvants alum and MF59 induce rapid recruitment of neutrophils and monocytes that participate in antigen transport to draining lymph nodes. Vaccine 2011;29:1812–23.
[8] Castellino F, Huang AY, Altan-Bonnet G, Stoll S, Scheinecker C, Germain RN. Chemokines enhance immunity by guiding naive CD8+ T cells to sites of CD4+ T cell-dendritic cell interaction. Nature 2006;440:890–5.
[9] Chen J, Yu X, Zheng Q, Hou L, Du L, Zhang Y, et al. The immunopotentiator CVC1302 enhances immune efficacy and protective ability of foot-and-mouth disease virus vaccine in pigs. Vaccine 2018;36:7929–35.
[10] Coppotelli G, Ross J, Ling A, Kim K, Sinclair D. Cpne2: a new regulator of lysosomal-mitochondrial function involved in aging and disease. Innovation in aging 2018;2:387–8.
[11] Cox SJ, Barnett PV. Experimental evaluation of foot-and-mouth disease vaccines for emergency use in ruminants and pigs: a review. Vet Res 2009;40:13.
[12] Das A, Dinh PX, Pattnaik AK. Trim21 regulates Nmi-IFI35 complex-mediated inhibition of innate antiviral response. Virology 2015;485:383–92.
[13] Du L, Chen J, Hou L, Yu X, Zheng Q, Hou J. Long-term humoral immunity induced by CVC1302-adjuvanted serotype O foot-and-mouth disease inactivated vaccine correlates with promoted T follicular helper cells and thus germinal center responses in mice. Vaccine 2017;35:7088–94.
[14] Du L, Pang F, Yu Z, Xu X, Fan B, Huang K, et al. Assessment of the efficacy of two novel DNA vaccine formulations against highly pathogenic Porcine Reproductive and Respiratory Syndrome Virus. Sci Rep 2017;7:41886.
[15] Dupont N, Nascimbeni AC, Morel E, Codogno P. Molecular mechanisms of noncanonical autophagy. Int Rev Cell Mol Biol 2017;328:1–23.
[16] Dupuis M, Denis-Mize K, Labarbara A, Peters W, Charo IF, Mcdonald DM, et al. Immunization with the adjuvant MF59 induces macrophage trafficking and apoptosis. Eur J Immunol 2001;31:2910–8.
[17] Eberlein J, Nguyen TT, Victorino F, Golden-Mason L, Rosen HR, Homann D. Comprehensive assessment of chemokine expression profiles by flow cytometry. J Clin Invest 2010;120:907–23.
[18] Genestier L, Taillardet M, Mondiere P, Gheit H, Bella C, Defrance T. TLR agonists selectively promote terminal plasma cell differentiation of B cell subsets specialized in thymus-independent responses. J Immunol 2007;178:7779–86.
[19] Germain C, Meier A, Jensen T, Knapnougel P, Poupon G, Lazzari A, et al. Induction of lectin-like transcript 1 (LLT1) protein cell surface expression by pathogens and interferon-gamma contributes to modulate immune responses. J Biol Chem 2011;286:37964–75.
[20] Golde WT, Pacheco JM, Duque H, Doel T, Penfold B, Ferman GS, et al. Vaccination against foot-and-mouth disease virus confers complete clinical protection in 7 days and partial protection in 4 days: Use in emergency outbreak response. Vaccine 2005;23:5775–82.
[21] Grubman MJ, Baxt B. Foot-and-mouth disease. Clin Microbiol Rev 2004;17:465–93.
[22] Hou J, Wang T, Xie Q, Deng W, Yang JY, Zhang SQ, et al. N-Myc-interacting protein (NMI) negatively regulates epithelial-mesenchymal transition by inhibiting the acetylation of NF-kappaB/p65. Cancer Lett 2016;376:22–33.
[23] Kanda T, Ozawa M, Tsukiyama-Kohara K. IRES-mediated translation of foot-and-mouth disease virus (FMDV) in cultured cells derived from FMDV-susceptible and -insusceptible animals. BMC Vet Res 2016;12:66.
[24] Kasturi SP, Skountzou I, Albrecht RA, Koutsonanos D, Hua T, Nakaya HI, et al. Programming the magnitude and persistence of antibody responses with innate immunity. Nature 2011;470:543–7.
[25] Llibre A, Lopez-Macias C, Marafioti T, Mehta H, Partridge A, Kanzig C, et al. LLT1 and CD161 Expression in Human Germinal Centers Promotes B Cell Activation and CXCR4 Downregulation. J Immunol 2016;196:2085–94.
[26] Maglione PJ, Simchoni N, Cunningham-Rundles C. Toll-like receptor signaling in primary immune deficiencies. Ann N Y Acad Sci 2015;1356:1–21.
[27] Mathew SO, Chaudhary P, Powers SB, Vishwanatha JK, Mathew PA. Overexpression of LLT1 (OCIL, CLEC2D) on prostate cancer cells inhibits NK cell-mediated killing through LLT1-NKRP1A (CD161) interaction. Oncotarget 2016;7:68650–61.
[28] Mihaylova MM, Shaw RJ. The AMPK signalling pathway coordinates cell growth, autophagy and metabolism. Nat Cell Biol 2011;13:1016–23.
[29] Puri C, Renna M, Bento CF, Moreau K, Rubinsztein DC. Diverse autophagosome membrane sources coalesce in recycling endosomes. Cell 2013;154:1285–99.
[30] Rodriguez LL, Gay CG. Development of vaccines toward the global control and eradication of foot-and-mouth disease. Expert Rev Vaccines 2011;10:377–87.
[31] Rodriguez LL, Grubman MJ. Foot and mouth disease virus vaccines. Vaccine 2009;27(Suppl 4):D90–4.
[32] Rohrbach TD, Shah N, Jackson WP, Feeney EV, Scanlon S, Gish R, et al. The Effector Domain of MARCKS Is a Nuclear Localization Signal that Regulates Cellular PIP2 Levels and Nuclear PIP2 Localization. PLoS ONE 2015;10:e0140870.
[33] Rubtsov AV, Swanson CL, Troy S, Strauch P, Pelanda R, Torres RM. TLR agonists promote marginal zone B cell activation and facilitate T-dependent IgM responses. J Immunol 2008;180:3882–8.
[34] Sajadi SM, Mirzaei V, Hassanshahi G, Khorramdelazad H, Daredor HY, Hosseini SM, et al. Decreased expressions of Toll-like receptor 9 and its signaling molecules in chronic hepatitis B virus-infected patients. Arch Pathol Lab Med 2013;137:1674–9.
[35] Schenten D, Medzhitov R. The control of adaptive immune responses by the innate immune system. Adv Immunol 2011;109:87–124.
[36] Seubert A, Monaci E, Pizza M, O'hagan DT, Wack A. The adjuvants aluminum hydroxide and MF59 induce monocyte and granulocyte chemoattractants and enhance monocyte differentiation toward dendritic cells. J Immunol 2008;180:5402–12.
[37] Shapiro-Shelef M, Calame K. Regulation of plasma-cell development. Nat Rev Immunol 2005;5:230–42.
[38] Slattery ML, Lundgreen A, Herrick JS, Wolff RK. Genetic variation in RPS6KA1, RPS6KA2, RPS6KB1, RPS6KB2, and PDK1 and risk of colon or rectal cancer. Mutat Res 2011;706:13–20.
[39] Spaggiari GM, Abdelrazik H, Becchetti F, Moretta L. MSCs inhibit monocyte-derived DC maturation and function by selectively interfering with the generation of immature DCs: central role of MSC-derived prostaglandin E2. Blood 2009;113:6576–83.
[40] Thomas EC, Hook SC, Gray A, Chadt A, Carling D, Al-Hasani H, et al. Isoform-specific AMPK association with TBC1D1 is reduced by a mutation associated with severe obesity. Biochem J 2018;475:2969–83.
[41] Wang J, Yang B, Hu Y, Zheng Y, Zhou H, Wang Y, et al. Negative regulation of Nmi on virus-triggered type I IFN production by targeting IRF7. J Immunol 2013;191:3393–9.
[42] Webster CP, Smith EF, Bauer CS, Moller A, Hautbergue GM, Ferraiuolo L, et al. The C9orf72 protein interacts with Rab1a and the ULK1 complex to regulate initiation of autophagy. EMBO J 2016;35:1656–76.
[43] Wisniewski JR, Zougman A, Nagaraj N, Mann M. Universal sample preparation method for proteome analysis. Nat Methods 2009;6:359–62.
[44] Xu X, Zhu Q, Zhang R, Wang Y, Niu F, Wang W, et al. ITRAQ-Based Proteomics Analysis of Acute Lung Injury Induced by Oleic Acid in Mice. Cell Physiol Biochem 2017;44:1949–64.
[45] Yu Y, Liu D, Liu Z, Li S, Ge Y, Sun W, et al. The inhibitory effects of COL1A2 on colorectal cancer cell proliferation, migration, and invasion. J Cancer 2018;9:2953–62.
[46] Yuan HX, Russell RC, Guan KL. Regulation of PIK3C3/VPS34 complexes by MTOR in nutrient stress-induced autophagy. Autophagy 2013;9:1983–95.
[47] Zhao YG, Liu N, Miao G, Chen Y, Zhao H, Zhang H. The ER Contact Proteins VAPA/B Interact with Multiple Autophagy Proteins to Modulate Autophagosome Biogenesis. Curr Biol 2018;28(1234–1245):e1234.